THE JOURNAL OF BIOLOGICAL CHEMISTRY
Vol. 273, No. 45, Issue of November 6, pp. 30046–30055, 1998

Printed in U.S.A.

Role of the Putative Zinc Finger Domain of *Saccharomyces cerevisiae* DNA Polymerase ϵ in DNA Replication and the S/M Checkpoint Pathway*

(Received for publication, June 8, 1998, and in revised form, August 26, 1998)

Rajiv Dua, Daniel L. Levy, and Judith L. Campbell‡

From Braun Laboratories 147-75, California Institute of Technology, Pasadena, California 91125

It has been proposed that C-terminal motifs of the catalytic subunit of budding yeast polymerase (pol) ϵ (*POL2*) couple DNA replication to the S/M checkpoint (Navas, T. A., Zheng, Z., and Elledge, S. J. (1995) *Cell* 80, 29–39). Scanning deletion analysis of the C terminus reveals that 20 amino acid residues between two putative C-terminal zinc fingers are essential for DNA replication and for an intact S/M cell cycle checkpoint. All mutations affecting the inter-zinc finger amino acids or the zinc fingers themselves are sensitive to methylmethane sulfonate and have reduced ability to induce *RNR3*, showing that the mutants are defective in the transcriptional response to DNA damage as well as the cell cycle response. The mutations affect the assembly of the pol ϵ holoenzyme. Two-hybrid assays show that the *POL2* subunit interacts with itself, and that the replication and checkpoint mutants are specifically defective in the interaction, suggesting (but not proving) that direct or indirect dimerization may be important for the normal functions of pol ϵ. The *POL2* C terminus is sufficient for interaction with *DPB2*, the essential and phylogenetically conserved subunit of pol ϵ, but not for interaction with *DPB3*. Neither Dpb3p nor Dpb2p homodimerizes in the two-hybrid assay.

Yeast mutants with defects in S phase progression normally arrest their cell cycles before entering mitosis. This arrest is attributed to a surveillance mechanism, called the S/M checkpoint pathway, that prevents inappropriate segregation of unreplicated or damaged chromosomes by monitoring some as yet ill defined aspect of chromosome structure. In the presence of damage, a signal is generated and transmitted either to the cell cycle apparatus, resulting in inhibition of cell cycle progression, or to the cellular transcription apparatus, resulting in induction of functions that participate in repair of the defect and/or delay cell cycle progression (1). In addition to the S/M checkpoint pathway, there are at least three other checkpoint pathways that have the replication apparatus either as a target of inhibition (G_1/S) or as a sensor of aberrant function (S/M) or both (intra-S) (2–4). However, information about the mechanism linking DNA replication and either the cell cycle apparatus or the transcription apparatus in these checkpoints has been limited. Several years ago, it was shown that certain DNA replication initiation mutants, in addition to failing to enter S phase, also fail to establish the S/M checkpoint (5, 6). Such mutants, rather than arresting the cell cycle, progress into mitosis with unreplicated chromosomes, divide and die. It was proposed that assembly of the replication apparatus may be required to establish the checkpoint and that one or more component(s) of the assembled apparatus monitors the completeness of replication and sends an inhibitory signal to the cell cycle apparatus when there is unreplicated (or damaged) DNA (7). In keeping with this model, several mutants affecting proteins in the replisome were recently shown to be defective in the S/M checkpoint: *rfc2*, *rfc5*, *dpb11*, and *pol2* (8–12). *POL2* encodes the essential DNA polymerase, pol[1] ϵ, and Rfc2p, Rfc5p, and (probably) Dpb11p are polymerase accessory proteins. Thus, an enzyme that was originally thought to have an essential housekeeping function also seems to have an important regulatory function in the cell cycle. This dual function may form an important paradigm for other checkpoint pathways (13, 14).

The first checkpoint-deficient allele of *pol2* was identified in a screen for mutants defective in a transcriptional response observed when hydroxyurea is used to block DNA replication (15). (Hydroxyurea blocks DNA synthesis by inhibiting precursor biosynthesis and thus depleting nucleotide pools.) Wild-type cells treated with HU respond by inducing the *RNR3* gene, but one mutant, *dun2* (*d*amage *un*inducible), was deficient in induction (9). Cloning of the *DUN2* gene showed that it was identical to *POL2*. Two *pol2* mutants temperature-sensitive for DNA replication and DNA repair (16, 17) also turned out to be defective in the transcriptional response to DNA damage (9, 15). What was really interesting, however, was that the latter two mutants were also defective in the cell cycle response to HU inhibition, since they entered mitosis with incompletely replicated chromosomes. Further work showed that the Pol2 DNA damage response pathway appears to function in parallel to the Rad9 pathway and be specific for damage incurred or encountered during S phase (10). *POL2* seems to act upstream of *RAD53*, a protein kinase that is one of the central signal transducers in both the transcriptional and cell cycle responses to DNA damage, and therefore *POL2* has been proposed as a sensor of DNA damage and stalled replication forks. We have been interested in identifying new mutants affecting *POL2* to further define the mechanism by which pol ϵ participates in the S/M checkpoint.

pol ϵ is one of three essential DNA polymerases in yeast (16, 18, 19). pol ϵ is highly homologous to the other essential DNA polymerases, pol δ and pol α, in the catalytic domains, which have been shown to fall in the N-terminal and central portion

* This work was supported by PHS grant GM25508 and American Heart Association Research Fellowship Award 1153-F12. The costs of publication of this article were defrayed in part by the payment of page charges. This article must therefore be hereby marked "*advertisement*" in accordance with 18 U.S.C. Section 1734 solely to indicate this fact.

‡ To whom correspondence should be addressed. Tel.: 626-395-6053; Fax: 626-405-9452; E-mail: jcampbel@cco.caltech.edu.

[1] The abbreviations used are: pol, DNA polymerase; 5-FOA, 5-fluoroorotic acid; aa, amino acid; HU, hydroxyurea; MMS, methylmethane sulfonate; ZF1, 4-cysteine motif between aa 2103 and aa 2133; ZF2, 4-cysteine motif, between aa 2163 and aa 2183; HA, hemagglutinin; PCR, polymerase chain reaction.

TABLE I
Yeast strains

Strain	Genotype	Source
YHA1	*MATa/MATα POL2/pol2–3::LEU2 LEU2–3, 112/LEU2–3, 112 ura3–52 trp1–289 ade5–1/ADE5*	(19)
A1128	*MATa ade5–1 leu2–3, 112 ura3–52 trp1–289 pol2–3::LEU2* [YEpPOL2]	This study
YHA301	*MATa ade5–1 leu2–3, 112 ura3–52 pol2–3::LEU2* [YCp*pol2–18*]	(19)
YRD1	A1128/pk1	This study
YRD2	A1128/pk2	This study
YRD3	A1128/pk3	This study
YRD4	A1128/pk4	This study
YRD5	A1128/pk5	This study
YRD6	A1128/pk7	This study
YRD7	A1128/pk8	This study
YRD8	A1128/pk9	This study
YRD9	A1128/pk10	This study
YRD10	A1128/pk11	This study
YRD11	A1128/pk12	This study
YRD12	A1128/pk13	This study
PJ69–4A	*LYS2::GAL1-HIS3, GAL2-ADE2, met2::GAL7-lacZ*	(29)
SS111–2-11	*MATa, trp1–289, ura3–12, ade2–101, gal2, can1, pol2–11*	(16)
SS111–2-12	*MATa, trp1–289, ura3–12, ade2–101, gal2, can1, pol2–12*	(16)
TC102–2-11	*MATα, leu2, ura3–52, can1, pol2–11*	(16)
TC102–2-12	*MATα, leu2, ura3–52, can1, pol2–12*	(16)

of the proteins (20). The temperature-sensitive mutants, *pol2–9* and *pol2–18,* have mutations in the conserved catalytic polymerase domain, M643I and P710S, while mutations at Asp-290 and Glu-292 reduce the exonuclease proofreading activity and affect the fidelity of the polymerase (19). The Dun$^-$, DNA damage response-defective *pol2* mutants described above all map to the C terminus, while the N-terminal *pol2–9* and *pol2–18* mutants are proficient in the checkpoint. *pol1* and *pol3* mutants, defective in DNA polymerases α and δ, respectively, have constitutively elevated expression of the damage inducible genes, rather than a defect in induction (15).

What is special about the pol ϵ C terminus that could be important for both DNA replication and DNA damage sensing? Interestingly, the C-terminal region of pol ϵ is essential *in vivo*, though far removed from the catalytic domains (9). *In vitro*, however, the C-terminal mutants show nearly normal DNA polymerase activity (16). The catalytic site mutants, *pol2–9* and *pol2–18*, show interallelic complementation with the C-terminal domain mutants, *pol2–11* and *pol2–12*. It has been suggested therefore that the C- and N-terminal domains have two independent functions or that pol ϵ dimerizes and heterodimers are active. The most obvious structural feature of the C terminus is a cysteine-rich region, with two putative zinc finger motifs (ZF1 and ZF2, Fig. 1). The Dun$^-$ mutants, *pol2–11* and *pol2–12*, map 11 and 15 amino acids downstream of this region (9, 16). Since they are nonsense codons their phenotype could be due directly to loss of critical motifs within the downstream amino acids or to an indirect effect on the structure of the near-by cysteine-rich region (see Fig. 1). To identify the specific amino acids involved in sensing the replication block and DNA damage and the mechanism by which they induce the cell cycle and transcription responses, we constructed a series of site specific deletion mutants near the C terminus of pol ϵ. Here, we demonstrate that a cluster of 20 amino acid residues between the two putative zinc fingers is essential for replication *in vivo* and the S/M checkpoint. Using the yeast two-hybrid assay for protein/protein interaction, we discovered that the C terminus of pol ϵ can self-interact and that the replication- and checkpoint-defective mutants are also defective in the interaction. The C-terminal region is sufficient for interaction with Dpb2p, the second largest subunit of pol ϵ, and the mutations that abolish self-interaction also affect Dpb2p interaction.

EXPERIMENTAL PROCEDURES

Materials—plitmus39 vector and M13KO7 phage were from New England Biolabs. pRS314 *TRPARS1CEN4* vector was from the laboratory collection (21). pZZ2, carrying *RNR3-lacZ* was provided by Dr. Stephen Elledge (Baylor College of Medicine, Houston, TX). Restriction enzymes, T4 DNA ligase, Vent DNA polymerase, and Klenow large fragment were obtained from New England Biolabs. Mutagenesis kit was from Bio-Rad. All the oligonucleotides were synthesized by the oligonucleotide facility at Caltech. α factor, HU, MMS, *ortho*-nitrophenyl-β-D-galactopyranoside, ampicillin, and kanamycin were from Sigma. Plasmid preparation kits were from Qiagen. Standard medium for growth of bacteria and yeast was from Difco. pAS2–1 (binding domain) and pACT2 (activation domain) yeast two-hybrid vectors, Gal4BD antibody, and Gal4AD antibody were obtained from CLONTECH. ECL Western blotting reagents and nitrocellulose membrane were from Amersham Pharmacia Biotech. Monoclonal 12CA5 antibodies for the hemagglutinin epitope were prepared at Caltech. Monoclonal rat anti-tubulin antibody (clone YOL1/34) was from Accurate Chemical and Scientific Corp. Fluorescein-conjugated, goat anti-rat IgG secondary antibody was obtained from ICN Corp. Polyclonal antibody for the pol ϵ holoenzyme complex was provided by Dr. Akio Sugino (Osaka University, Osaka, Japan).

Bacterial and Yeast Strains—Escherichia coli CJ236 *dut-1, ung-1, thi-1, relA1;* pCJ105(Cm^r) was provided in the Bio-Rad mutagenesis kit. For routine cloning, the DH5α bacterial strain was obtained from Life Technologies, Inc. Yeast strains are listed in Table I.

Mutagenesis and Subcloning—pSEY18 vector containing the full-length *POL2* gene cloned at the *Sac*I site (16) was digested with *Bsr*GI, and the C-terminal *POL2* fragment (~2.3 kb) was purified. The purified C-terminal fragment was subcloned at the *Bsr*GI site in the pLitmus 39 phagemid vector (pLitPOL2). The linearized pSEY18 vector containing the N terminus of the *POL2* was self-ligated and digested with *Sac*I, and the *POL2* fragment was purified. It was then subcloned in the pRS314 vector (pRPOL2). pLitPOL2 was transformed into CJ236 *E. coli* strain, and transformed cells were infected with M13KO7 phage. Uracil-phagemid DNA template was prepared, and mutagenesis was performed according to instructions of the supplier (Bio-Rad) with some modifications. Briefly, the mutagenic oligonucleotide was annealed to the uracil-containing DNA template by first heating at 70 °C for 3 min and then slowly cooling to 30 °C for 1 h. The polymerization mix, T4 DNA ligase and T7 DNA polymerase were added to the annealed template and incubated on ice for 5 min, at room temperature for 5 min, and then at 37 °C for 4 h. The reaction was stopped by adding 17 μl of 1× TE buffer. 3 μl of the final mixture was transformed into DH5α cells. The DNA was prepared from the transformants and sequenced using automated sequencing at the Caltech DNA sequencing facility. The oligonucleotides used for the mutagenesis are as follows: Δ2213–2222, 5′-GCG TTA TAT ACT GCT TAC TCA TAT ATC AAA ACC GTA ATA CTT G-3′; Δ2203–2212, 5′-ATC AGC AAT ACA ACT CAA TAA CTT

AAA CAC ATT TAA CTT TTG-3′; Δ2193–2197, 5′-C TTG CTT AAA CAC ATT TAA TTC TCT GGG GAG AGTTCC-3′; Δ2183–2192, 5′-ATT TAA CTT TTG AAC AAT GCT GGC ACA TGG ACA GTG GGC AC-3′; Δ2173–2182, 5′-GAG AGT TCC TTC CCA CGC GCC ACG TTT CAC TTT ATG ACA TCT G-3′; Δ2163–2172, 5′-CAG TGG GCA CTC ATA TAG TCC AAA TCT TGA ATT AAA TAG G-3′; Δ2153–2162, 5′-CTT TAT GAC ATC TGG AGC ATC TAG AAC GTA GTT TTT GAA TCA G-3′; △2143–2152, 5′-GAA TTA AAT AGG ATT CGA TAT CCA ACA ATA CTT GAT TAA AGG C-3′; Δ2133–2142, 5′-GTT TTT GAA TCA GGT GTT CTT GTC TGA CGC ATG AAA AAA TAG-3′; Δ2123–2132, 5′-C TTG ATT AAA GGC TTT GTG ACA TGC CTT ACA AAA GTC AAT ATC-3′; Δ2113–2122, 5′-GAA AAA ATA GAT TCA GGA GCA AAA CAG TAT TCA CAT AAA AAA TC-3′; Δ2103–2112, 5′-CAA AAG TCA ATA TCA GAA ATG AAC ACG AGA CTA AAA CTT GGA TC-3′; R2163-STOP, 5′-GAC ATC TGG ATT ATC TCA AAT CTT G-3′; R2151-STOP, S2152-STOP, 5′-GA TTC GAT ATC TCA TCA TAG TTT TTG AAT C-3′; V2103-STOP, 5′-CCA TAA AAA GGA TCC TTA CAC GAG-3′; F2093-STOP, K2094-STOP, 5′-CAA ACT TGG ATC TCA TCA TTC CGC TAC-3′; D2192-STOP, 5′-G AAC AAT GCT TTA TCT GGG GAG-3′ (*pol2–11*); Q2196-STOP, 5′-C ATT TAA CTT TTA AAC AAT GC-3′ (*pol2–12*); P710S, 5′-GTT TTT GTT GGA AA AGT CTC ATT-3′ (*pol2–18*).

The full-length *POL2* gene was reconstituted by subcloning the mutant *pol 2* C terminus fragments into the pRPOL2 vector at the *Bsr*GI site. The recombinants were screened using colony hybridization. The orientation of the cloned insert was confirmed using *Mfe*I digestion and by DNA sequencing. *pol2–11*, *pol2–12*, and *pol2–18* were made by site-directed mutagenesis to ensure that the phenotype of the original mutations was due to the single base pair changes found in the original mapping. The plasmids are listed in Table II. The size of the expressed proteins was determined by Western blotting after subcloning the C-terminal regions into the two-hybrid assay vectors described below. These experiments verified that the stop codons introduced were effective in truncating the proteins at the desired positions.

Plasmid Shuffling—The plasmid shuffling assay was done as described (16, 22). The *pol2*Δ strain containing wild-type *POL2* on a *URA* vector (pSEY18) was transformed with wild-type and mutant genes in the pRS314 Trp^+ vector (pk series plasmids). Transformants were assayed for viability on synthetic agar plates lacking tryptophan in the presence of 5-FOA at 24 °C and 37 °C.

Sensitivity of pol2 Mutants to MMS—Fresh YPD agar plates were made with MMS with varying concentration. The *pol2* mutant yeast strains (see Fig. 1) were grown at 24 °C to saturation in YPD medium, washed in sterile water, then serially diluted in 10-fold steps to 10^{-3}. Samples (5 μl) of each dilution were placed on the MMS plates and incubated at 24 °C for 4 days.

Induction of RNR3 Expression in the Presence of MMS—The *pol 2* yeast strains were transformed with pZZ2, which carries *RNR3-lacZ* (15). The yeast strains containing the *RNR3-lacZ* reporter were grown at 24 °C in selective medium until the A_{600} reached 0.6. The culture was divided in two equal halves. To one part, MMS was added to a final concentration of 0.01%. Both cultures were grown for another 6 h at 24 °C. The cells were washed once with water, and then β-galactosidase assays were carried out as per instructions (CLONTECH Matchmaker two-hybrid system manual).

Yeast Two-hybrid Protein-Protein Interaction Assay—Gal4-binding domain (Gal4-BD) plasmid pAST2–1 and Gal4-activation domain (Gal4-AD) plasmid pAST2–1 (Matchmaker two-hybrid system; CLONTECH) were used for cloning of the various genes. The PJ69–4A yeast strain (23) with three different reporters (*ADE2*, *HIS3*, *lacZ*), each under the control of a different promoter (*GAL2*, *GAL1*, and *GAL7*) was used for assessing the protein-protein interactions. To clone the C terminus (aa 1265–2222) of *POL2* in frame with the Gal4BD or GAl4AD, PCR was performed using primers with flanking *Nco*I and *Bam*HI sites. pK series plasmids (see Table II) containing the full-length wild-type and mutant *pol2* genes were used as the DNA template. Vent DNA polymerase was used for the PCR reactions. PCR products were purified from gels and ligated to *Nco*I/*Bam*HI-digested Gal4-BD and Gal4-AD vectors. The in-frame sequence near the N terminus was confirmed by sequencing.

The PJ69–4A yeast strain was co-transformed with the Gal4-BD and Gal4-AD fusion constructs using the polyethylene glycol/lithium acetate method. Transformed cells were selected on Trp^-/Leu^-/Ade^- synthetic agar plates at 30 °C for 4 days. Transformed cells were further screened on Trp^-/Leu^-/His^- synthetic agar plates containing 1 mM 3-amino-1,2,4-triazole at 30 °C for 3 days. Finally, the cells that grew on both Trp^-/Leu^-/Ade^- and Trp^-/Leu^-/His^- plates were quantitatively tested for β-galactosidase activity as per instructions (CLONTECH). The units of β-galactosidase activity were calculated according to β-galactosidase activity = $1000 \times A_{420}/(t \times v \times A_{600})$, where t = time (min) required for the reaction and $v = 0.1 \times$ concentration factor. To verify the expression of the Gal4-BD and Gal4-AD (with HA epitope on the N terminus) fusion proteins, Western blots were prepared using whole cell extracts as the source of protein and Gal4-BD antibody and 12CA5 antibodies, respectively, as probes.

DPB2 (24) and DPB3 (25) were cloned by PCR using yeast genomic DNA as a template, and expression was verified using 12CA5 antibody and polyclonal antibody to Dpb2p and Dpb3. The sequence of the oligonucleotides is shown below: DPB2, R1 (5′-CTT TAA AGT TTG GCC ATG GAA CTA G-3′) and R2 (5′-G TTC TTA TTT GGA TCC ATT ATT TAG-3′); DPB3, R3 (5′-C GGG CGC GCC ATG GAA ATG TCC AAC-3′) and R4 (5′-GTA CCG CAT GGA TCC AGA TCA C-3′).

TABLE II
Plasmids

Plasmid	Relevant genotype	Mutant	Base plasmid
pk1	*TRP1 ARS4 CEN6 POL2*		pRS314
pk2	*TRP1 ARS4 CEN6 pol2(Δ2103–2112)*	A	pRS314
pk3	*TRP1 ARS4 CEN6 pol2(Δ2113–2122)*	B	pRS314
pk4	*TRP1 ARS4 CEN6 pol2(Δ2123–2132)*	C	pRS314
pk5	*TRP1 ARS4 CEN6 pol2(Δ2133–2142)*	D	pRS314
pk6	*TRP1 ARS4 CEN6 pol2(Δ2143–2152)*	E	pRS314
pk7	*TRP1 ARS4 CEN6 pol2(Δ2153–2162)*	F	pRS314
pk8	*TRP1 ARS4 CEN6 pol2(Δ2163–2172)*	G	pRS314
pk9	*TRP1 ARS4 CEN6 pol2(Δ2173–2182)*	H	pRS314
pk10	*TRP1 ARS4 CEN6 pol2(Δ2183–2192)*	I	pRS314
pk11	*TRP1 ARS4 CEN6 pol2(Δ2193–2197)*	J	pRS314
pk12	*TRP1 ARS4 CEN6 pol2(Δ2203–2212)*	K	pRS314
pk13	*TRP1 ARS4 CEN6 pol2(Δ2213–2222)*	L	pRS314
pk14	*TRP1 ARS4 CEN6pol2(F2093-TAA)*		pRS314
pk15	*TRP1 ARS4 CEN6pol2(R2151-TAA)*		pRS314
pk16	*URA3 ARS4 CEN6(pol2–18)*		pRS316

RESULTS

Amino Acid Residues between ZF1 and ZF2 in the C Terminus of pol ϵ Are Essential for Viability—In order to better understand the molecular details of the C terminus of pol ϵ required for its role in DNA replication and damage sensing, we constructed a panel of deletion mutants covering the C-terminal 120 aa of the Pol2p protein and studied various phenotypes. (For clarity, we will refer in the text to the amino acid motifs in the region as they are defined in Fig. 1, although there are no structural data to support the designation "zinc finger" as yet.) Each mutant (Fig. 1, *A–L*) contains a deletion of 10 amino acids. Mutants A, B, C, and D have deletions in ZF1; mutants E and F have deletions between ZF1 and ZF2; mutants G and H have deletions in ZF2; and mutants I, J, K, and L have mutations in the extreme C terminus of pol ϵ. The previously studied *pol2–11* and *pol2–12* nonsense alleles fall in the region covered by deletion J. In addition to the deletion mutations, *pol2–11*, *pol2–12*, and *pol2–18* were remade by site-directed mutagenesis to ensure that the phenotype of the original mutations was due to the single base pair changes found in the original mapping. We first examined the ability of the mutants to complement a *pol2*Δ strain using a plasmid shuffling assay (16, 22). The mutant genes, cloned on a plasmid carrying a *TRP* selection marker, were transformed into a *pol2*Δ yeast strain, which was kept alive by the presence of a wild-type *POL2* gene on a *URA* plasmid. Transformants were analyzed for growth at 24 °C and 37 °C on synthetic agar medium containing 5-FOA, which is toxic to Ura^+ cells and therefore selects against cells carrying the wild-type *POL2* plasmid (Fig. 1). Among the mutants studied, mutants E and F showed a drastic growth defect when present as the only copies of the *pol2* gene in the cells. Mutant E was unable to support growth at any temperature, while mutant F was viable at 24 °C but inviable at 37 °C. Mutant F also grew slower than wild-type and was enlarged at 24 °C. Mutants A, B, C, and D showed a

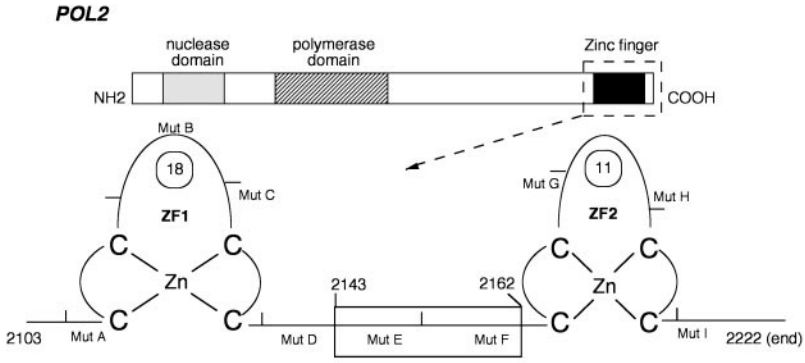

	Mutant	Mutation	Growth(+FOA) 25°C	37°C
	Wild type		+++	+++
	pol2-11	E2192-stop	++	-
	pol2-12	Q2196-stop	++	-
deletions in ZF1	A	Δ2103-2112	++	++
	B	Δ2113-2122	++	++
	C	Δ2123-2132	++	++
	D	Δ2133-2142	++	++
deletions between ZF1 and ZF2	E	Δ2143-2152	-	-
	F	Δ2153-2162	+/-	-
deletions in ZF2	G	Δ2163-2172	+++	+++
	H	Δ2173-2182	+++	+++
deletions in the extreme C-terminus	I	Δ2183-2192	+++	+++
	J	Δ2193-2197	+++	+++
	K	Δ2203-2212	+++	+++
	L	Δ2213-end	+++	+++

FIG. 1. **Site-specific mutagenesis in the C terminus of *POL2*.** The drawing shows the C terminus of *POL2* containing two putative zinc fingers. The *pol2* mutants were generated by using Kunkel's method as described in Experimental Procedures. Each site-specific mutant (A-L) contains a deletion of 10 consecutive amino acid residues as indicated. To test the effect of *pol2* mutations, the pRS314 (*Trp, CEN*) vector containing the mutant *pol2* genes (pk plasmids listed in Table II) was transformed into the strain A1128 *pol2–3::LEU2* [YEpPOL2], a haploid derivative of strain YHA1 at 24 °C. The transformants were replica plated onto agar plates lacking tryptophan and containing 5-FOA and incubated at 24 °C and 37 °C for 3–4 days. The symbols +++, ++, ±, - refer to normal growth, slow growth, very slow growth and no growth, respectively. The position of mutations E and F, between the two putative zinc fingers, is highlighted by a box.

marginal decrease in viability while mutants G, H, I, J, K, and L had no detectable growth defect. The results show that the mutations between ZF1 and ZF2 are critical for the essential role of pol ϵ in the cell.

Mutants *pol2–18* and *pol2–11*, with N- and C-terminal mutations, respectively, show interallelic complementation of their growth defect (9). Mutant F was therefore tested for complementation of *pol2–18* (and *pol2–11*) strains. Plasmid pk16 (*pol2–18*) was transformed into strain A1128/pk7 (*pol2-F*). Transformants were obtained but grew slowly at 37 °C, producing cultures that consisted of about 70% viable cells. Thus, *pol2-F* and *pol2–18* showed partial complementation. Neither mutant E nor mutant F complemented strain SS111*pol2–11.* Mutants A to D and G to L complemented *pol2–11*, as expected, since they themselves had only slight growth defects.

Mutant F Is Defective in the S/M Checkpoint—Cells defective in the S/M phase checkpoint progress into mitosis with incompletely replicated DNA resulting in rapid loss of cell viability. To address the role of the region between ZF1 and ZF2 in the S/M checkpoint, mutant F was examined for viability, DNA content, and nuclear and spindle morphology after incubation at the nonpermissive temperature. Wild-type and mutant F cells were grown to log phase at 24 °C and transferred to 37 °C, and samples of cells were collected at various time intervals and plated at 24 °C. As expected for a checkpoint defect, mutant F showed a 70% loss in viability compared with wild-type after 2 h at 37 °C, and 90% of the cells were dead after 4 h (Fig. 2*A*). The DNA content of the cells was also monitored at each time point. Mutant F cells accumulate in S phase (70%) and G_2 (30%) at 24 °C, which indicates a defect in S phase progression even at the permissive temperature (Fig. 2*B*, *0 h*). After 2 h at 37 °C, when the cell viability had dropped drastically, most cells revealed a DNA content between 1C and 2C, indicating a block in S phase. Nevertheless, about 40% of the cells had fragmented DNA or nuclear bodies (Fig. 2*C*) and partially elongated spindles (Fig. 2*C*). After 4 h, some cells had apparently undergone an abnormal mitosis as cells were present with both 1C and greater DNA content and again spindles were elongated and nuclei fragmented (Fig. 2*C*). Loss of viability and spindle elongation in the presence of unreplicated DNA are two phenotypes associated with a defect in the S/M checkpoint.

Since HU prevents cells from completing replication, HU can be used to monitor S/M checkpoint defects. Cells with an intact checkpoint arrest with short spindles and do not enter mitosis when treated with HU, thus recovering when HU is removed. Checkpoint mutants are supersensitive to HU because they enter mitosis with unreplicated DNA. The mutant strains were streaked on YPD plates containing 150 mM HU and incubated at 24 °C. Mutant F and *pol2–11* were inviable in the presence of HU even at 24 °C. Among the other mutants, A through D showed growth retardation, while the remaining *pol2* mutants did not show a significant growth defect relative to wild-type

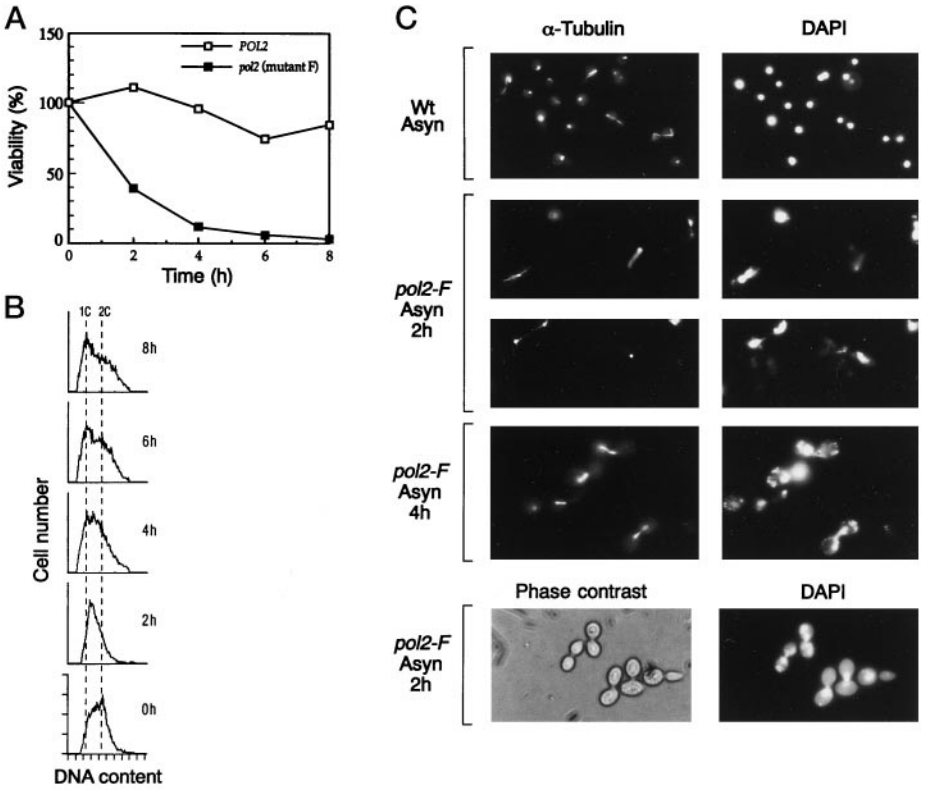

FIG. 2. **Behavior of *pol2* mutant F at the nonpermissive temperature.** *A*, cell viability. Asynchronous *POL2* wild-type and *pol2* mutant F cells were grown at 24 °C in YPD medium (pH 3.9) until mid-log phase (A_{600} = 0.6) and then shifted to 37 °C. Viability was determined by plating at 24 °C. *B*, DNA content. Samples were withdrawn at the indicated times, fixed in ethanol, digested with RNase and stained with propidium iodide (41). *C*, nuclear and spindle morphology. After 2 and 4 h, *pol2* mutant F cells were fixed in ethanol (for nuclear morphology) or formaldehyde (for tubulin morphology). The nucleoid was observed using 4′,6-diamino-2-phenylindole (*DAPI*), and spindle morphology was determined using anti-α-tubulin antibody (9, 42, 43).

(data not shown).

Because of its supersensitivity to HU, mutant F was further examined for viability, DNA content, and nuclear and spindle morphology after treatment with HU at the nonpermissive temperature. Wild-type and mutant F cells were arrested in the G_1 phase using α-factor. They were then shifted to 37 °C, and half of the culture was incubated in the continued presence of pheromone while the other half was released from the G_1 block in the presence of HU (26). Fig. 3*A* shows that mutant F incubated at the nonpermissive temperature during a sustained G_1 block retains viability. Thus, entry into S phase seems to be required to observe loss of viability (compare Figs. 2*A* and 3*A*). In contrast, mutant F cells released from the G_1 block and allowed to proceed into a synchronous S phase in the presence of HU at the nonpermissive temperature show a significant loss of viability compared with wild-type (Fig. 3*B*). Flow cytometric analysis of mutant and wild-type cells treated in the same fashion showed that both wild-type and mutant F cells were efficiently blocked in the S phase (DNA content between 1C and 2C) 4 h after release from the α-factor block into HU (Fig. 3*C*). Indirect immunofluorescence demonstrated that 60–70% of the mutant F cells had partially elongated spindles after 4 h in HU at the nonpermissive temperature (Fig. 3*D*), despite failure to complete replication (Fig. 3*C*), whereas wild-type cells showed no spindle separation (Fig. 3*D*). Asynchronous cultures of mutant F treated with HU also lose viability (Fig. 3*B*). Thus, there is a correlation between spindle elongation and loss of viability, indicative of a defective S/M checkpoint. This defect is observed only in cells incurring damage during S phase, but not in cells that are arrested in G_1, consistent with the results obtained for *pol2–11* (10). When released from α-factor block at the permissive temperature, mutant F did not show a significant loss in viability, even in the presence of HU (data not shown), which is consistent with the fact that the previously studied *pol2–11* also has a greater defect in the S/M checkpoint at elevated temperature (10). We conclude that mutant F is defective in the checkpoint pathway that monitors damage due to reduction of nucleotide pools as well as damage due to a thermolabile DNA polymerase at the nonpermissive temperature.

Mutations in ZF1 and between ZF1 and ZF2 Are Sensitive to Growth in the Presence of MMS—In order to study the effect of the *pol2* mutations on the DNA damage response, ability to tolerate MMS damage was monitored by examining growth of *pol2* mutants during chronic exposure to MMS. The mutants were grown to saturation at the permissive temperature, and various dilutions were placed on plates containing different concentrations of MMS. *pol2–11* and mutants A, B, D, and F showed greater sensitivity to 0.025% MMS in comparison to wild-type and mutants G and H at the permissive temperature (Fig. 4*A*). At 37 °C, mutants G and H also displayed MMS sensitivity (Fig. 4*B*). The results suggest that ZF1 and amino acid residues between ZF1 and ZF2 play a primary role in MMS sensitivity, while ZF2 may have a secondary role. It should be noted that the N-terminal *pol2–18* mutant was also sensitive to MMS, which may reflect a defect in the repair machinery itself, since *pol2–18* mutants have been shown previously to be proficient in the checkpoint (Ref. 9; see also Fig. 5).

Mutations in ZF1 and between ZF1 and ZF2 Show Reduced Inducibility of RNR3 Expression in the Presence of MMS—To investigate whether the MMS sensitivity of the C-terminal mutants was due to a checkpoint defect, we studied the ability of the *pol2* mutants to induce transcription of *RNR3* in the presence of MMS (9). The mutants were transformed with an *RNR3-lacz* reporter plasmid, and the expression of *RNR3* was assayed. Mutants A, C, and F and *pol2–11* showed a reduced level of *RNR3* expression in the presence of MMS (Fig. 5), while mutants G, H, and L showed a similar level of *RNR3* expression as compared with wild-type *POL2*. *pol2–18* also showed wild-type levels of induction, as expected. The residual transcription induction observed in mutants A, C, and F and *pol2–11* is expected and is probably due to the Rad9 pathway. (Elegant

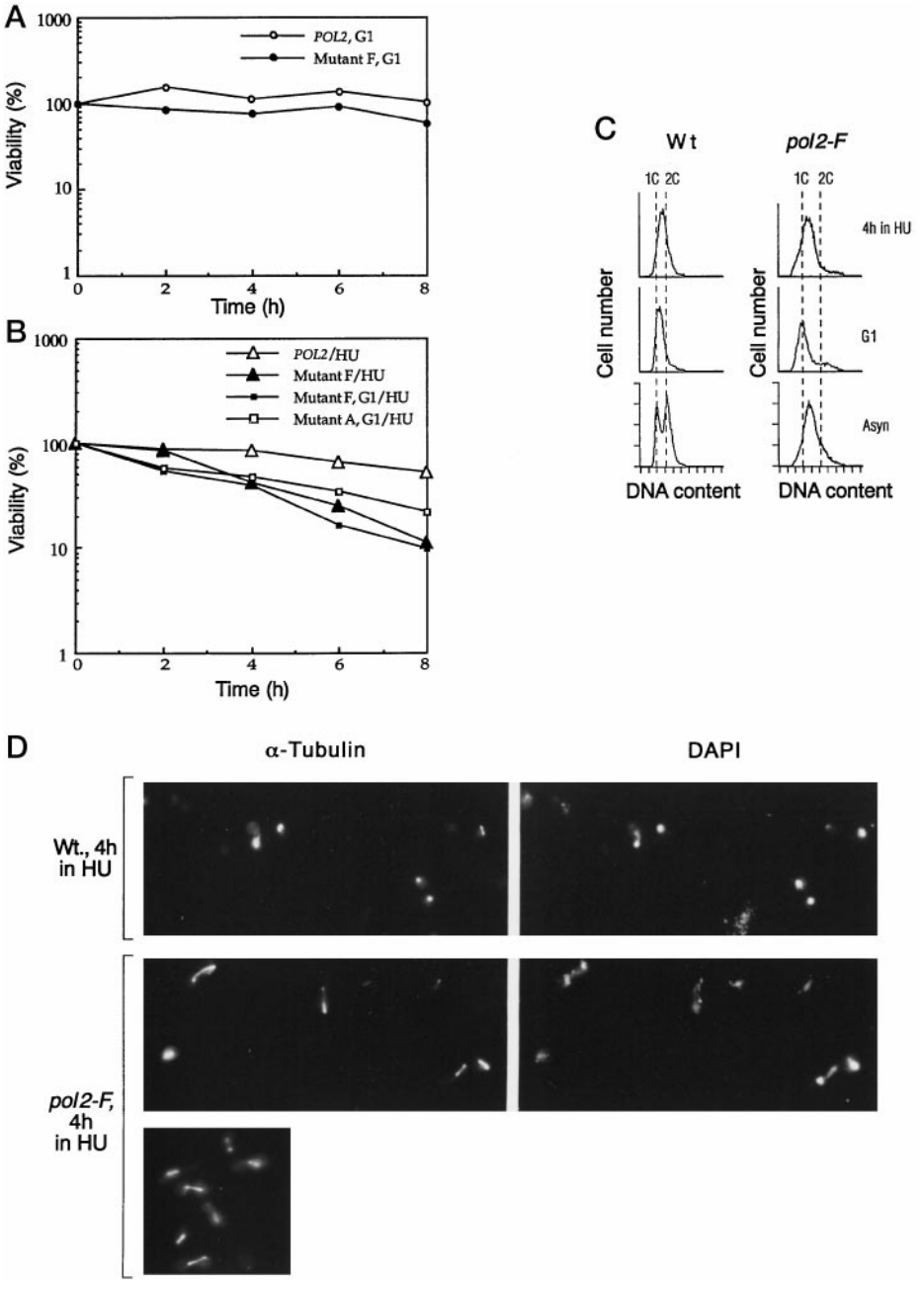

FIG. 3. **Cell cycle response of mutant F to HU.** *A*, viability of cells arrested at 37 °C in the presence of α factor. Cultures of wild-type and mutant F cells were adjusted to pH 3.9 and were treated with 8 μg/ml α-factor for 2 h at 24 °C. After 2 h, α factor was added again at 4 μg/ml and incubation continued for 2 h at 24 °C to achieve full arrest. The cultures were shifted to 37 °C and incubation continued for the indicated times. Additional α factor was added every 2 h to maintain the cells in G_1. *B*, viability of mutant F cells synchronized in G_1 and released into S phase in the presence of HU. For HU treatment of asynchronous cells, mid-log phase cells were transferred to YPD medium containing 0.2 M HU and shifted to 37 °C. Viability was determined by plating on medium lacking HU at 24 °C at various times as indicated. For synchronous cells, cultures were adjusted to pH 3.9 and were treated with 8 μg/ml α-factor for 4 h at 24 °C as described previously (9). (Additional α factor was added after 2 h.) After 4 h, α-factor was removed by washing. The cells were resuspended in medium prewarmed to 37 °C and containing 0.2 M HU. Viability was determined at the indicated times. Wild-type and mutant A (a ZF1 mutant) were treated in the same fashion as mutant F for comparison. *C*, DNA content of G_1 synchronized cells released into the cell cycle at 37 °C in the presence of 0.2 M HU. DNA content of the cells prepared as in *panel B* was determined as described in the legend to Fig. 2. *D*, nuclear and spindle morphology of cells from cultures analyzed in *panels B* and *C*. The nuclear morphology was visualized by 4′,6-diamino-2-phenylindole (*DAPI*), and spindle morphology was visualized using anti-α-tubulin antibodies as described in the legend to Fig. 2.

studies have recently dissected the damage response into two different branches and revealed that the Pol2 pathway responds to damage only during S phase, whereas Rad9 responds to damage in other phases of the cell cycle (10).) The results support the earlier proposal that the zinc fingers in the C terminus of pol ϵ act as a damage sensor and indicate that ZF1 may play a more important role than ZF2.

Since ZF1 showed greater MMS sensitivity while the inter-zinc finger mutants E and F showed greater sensitivity to HU, it seemed possible that the two different motifs might recognize different types of lesions. However, further examination of mutant A, which deletes two cysteines of ZF1, showed that it responded to HU with loss of viability at 37 °C just like mutant F (compare mutants A and F in Fig. 3*B*). Thus, ZF1 is not specific for MMS-induced damage.

Yeast Two-hybrid Assay of Protein Interactions in the C Terminus of POL2 with DPB2 and DPB3—The question now is how these motifs contribute to the checkpoint. Zinc finger domains have been inferred to play a critical role in protein-protein interactions (27). To test if the cysteine-rich C terminus of Pol2p is important for protein-protein interactions in pol ϵ, we employed the yeast two-hybrid assay (28) and investigated interactions among the subunits of pol ϵ: Pol2p, Dpb2p, and Dpb3p. The results are shown in Fig. 6 and Table III and are summarized in Table IV.

Since it had previously been proposed that pol ϵ might dimerize through the C terminus, we first checked self-interaction (9). We subcloned the C terminus (aa 1265-end) into two yeast expression vectors, one such that C terminus was in-frame with the Gal4 binding domain (pAST2–1) and another such that it was in-frame with Gal4 acidic activation domain (pACT2). The pACT2 activation domain vector also has an HA epitope toward the C terminus of Gal4. Both the vectors were co-transformed into yeast strain PJ69−4A, a strain that detects weak interactions and minimizes false positives (29). Interaction was assayed by the ability to transcribe three different reporters,

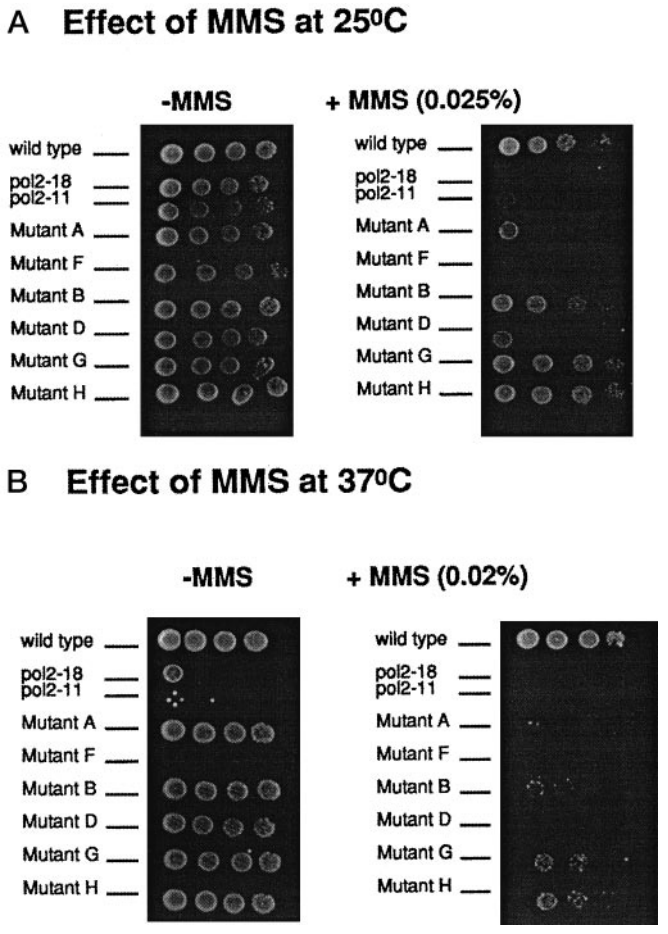

FIG. 4. **MMS sensitivity of mutants.** Cells were grown to saturation in YPD medium, washed in sterile water, then serially diluted in 10-fold steps to 10^{-3}. Aliquots (5 μl) of each dilution were placed on the MMS plate and incubated at 24 °C (*A*) and 37 °C (*B*) for 3–4 days.

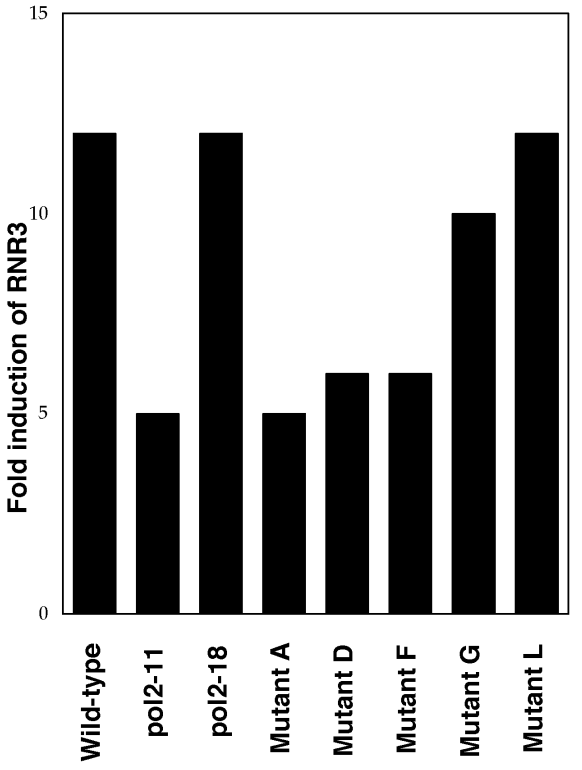

FIG. 5. **RNR3 expression by *pol2* mutants in the presence of MMS.** pol2 mutants were transformed with plasmid pZZ2 encoding the RNR3-lacZ fusion protein. The cells were analyzed for RNR3 expression as described under "Experimental Procedures" (9).

ADE2, HIS3, and *lacZ*, controlled by three different promoters, as described under "Experimental Procedures." The expression levels of the Gal4 fusion proteins were confirmed by Western blotting using anti-Gal4 binding domain and anti-HA 12CA5 antibodies. As shown in Fig. 6*A*, interaction was detected when the C terminus of pol ϵ was present on both binding domain and activation domain vectors. The C terminus of pol ϵ was unable to activate transcription on its own or in combination with control proteins p53 and T-antigen, suggesting that the self-association of pol ϵ through C terminus is specific. To localize the site of self-association, we subcloned various C-terminal mutants of pol ϵ in both binding domain and activation domain vectors and assayed for the protein-protein interactions. Deletion of the entire zinc finger region and the extreme C terminus (Δ2103-end) abolished interaction, while deletion of ZF2 and the extreme C terminus (Δ2163-end) did not, localizing the effect to the region containing ZF1 and amino acids between the two zinc fingers. Mutants A and H, with deletions within ZF1 and ZF2, respectively, showed interaction; but the replication/checkpoint-defective mutants E and F, with deletions between ZF1 and ZF2, failed to show any interaction. (Western blotting confirmed that the proteins were expressed efficiently (Fig. 6*B*).) Thus, there is a striking correlation between the mutants that affect replication and the S/M checkpoint and those that affect interaction as measured by the two-hybrid assay. With these experiments it is impossible to determine if the interaction documented is direct or indirect, however.

We next investigated interaction of Pol2p with the other pol ϵ subunits. We found that the C terminus interacts strongly with *DPB2* but is not sufficient for interaction with *DPB3* (Tables III and IV). Mutants E and F interact with *DPB2*, suggesting that the deletions do not cause a catastrophic disruption of the structure of the entire C-terminal region. However, quantitation of the interaction by β-galactosidase assay (Table III) suggests the interaction is weakened by the mutations. Deletions of the extreme C terminus such as are found in *pol2–11* and *pol2–12* also fail to abolish interaction with Dpb2p, but reduce the level of β-galactosidase activity. However, deletion of 30 amino acids between mutant F and mutant J, which includes ZF2, abolishes interaction. This may be due to a large structural perturbation, however, since mutants G, H, and I each appear to interact with *DPB2*. The interaction between the *POL2* C terminus and *DPB2* has been verified by expression in recombinant baculovirus infected insect cells, as has the reduced affinity between *pol2* mutant E and *DPB2*.[2] Since mutants E and F interact with *DPB2*, this may suggest that the effects on checkpoint are directly due to the mutations in *POL2* rather than indirectly due to failure to interact with another protein in the holoenzyme complex. On the other hand, the inefficient interaction with mutant E and Dpb2p may suggest the checkpoint defect reflects faulty assembly of the holoenzyme.

Neither Dpb2p nor Dpb3p appear to self-interact by the two-hybrid assay (Table IV).

DISCUSSION

Yeast DNA polymerase ϵ plays an essential role in chromosomal replication (16, 18, 19). In recent years, additional roles of pol ϵ in repair and cell-cycle regulation have emerged (9, 10, 17). Structure-function analysis has suggested that the C ter-

[2] R. Dua and J. L. Campbell, unpublished results.

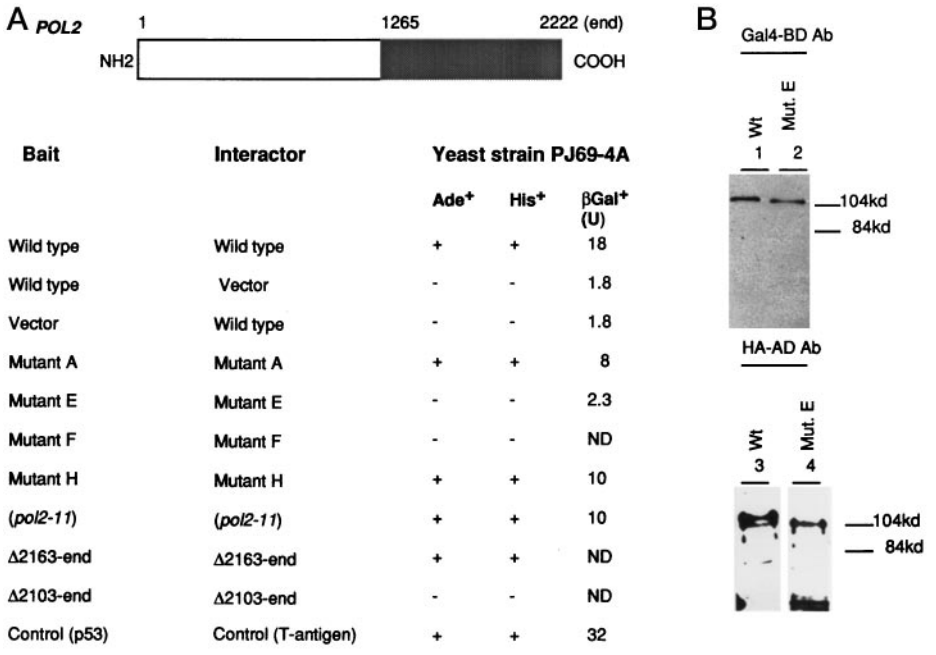

FIG. 6. **Yeast two-hybrid analysis.** *A*, interactions. The C terminus (aa1265-STOP) of *POL2* was prepared by PCR and cloned into pAS2–1 binding domain and pACT2 activation domain vectors as described under "Experimental Procedures." The resulting Gal4 fusion vectors were co-transformed into strain PJ69–4A. Ability to grow on medium lacking adenine or histidine was monitored. The β-galactosidase activity was measured using *ortho*-nitrophenyl-β-D-galactopyranoside as substrate, as described under "Experimental Procedures." The activity is expressed in β-galactosidase units. *B*, Western blots of extracts of cells expressing mutant E in the binding domain and activation domain vectors. Fusions in the binding domain vector were detected with Gal4 antibody, and fusions in the activation domain vector were detected with 12CA5 anti-hemagglutinin antibody as described under "Experimental Procedures." The band corresponding to mutant E migrates just above the 104-kDa marker.

TABLE III
Two-hybrid interaction between DPB2 and the POL2 C terminus

All *POL2* constructs represent C-terminal fusions beginning at aa 1265, as in Fig. 6.

Bait	Prey	Ade	His	β-Gal
				units
DPB2	*Vector*	−	−	2.2
DPB2	*DPB2*	−	−	ND
POL2(WT)	*DPB2*	+	+	28
DPB2	*POL2(WT)*	+	+	30
pol2(E)	*DPB2*	+	+	21
pol2(F)	*DPB2*	+	+	ND
pol2(G)	*DPB2*	+	+	ND
pol2(I)	*DPB2*	+	+	ND
pol2–11	*DPB2*	+	+	20
pol2(Δ2163-STOP)	*DPB2*	−	−	ND

TABLE IV
Summary of two-hybrid interactions between the C terminus of POL2 and its subunits, DPB2 and DPB3

Bait	Prey	Prey	Prey
	POL2(1265–2222)[a]	*DPB2*[b]	*DPB3*[b]
WT (1265–2222)	+	+	−
A	+	+	−
E	−	+	−
F	−	+	−
G	+	+	−
H	+	+	−
I	+	+	−
2192-STOP(pol2–11)	+	+	−
2163-STOP	+	−	−
2103-STOP	−	ND	ND
DPB2	+	−	−
DPB3	−	−	−

[a] All of the *POL2* genes used as prey correspond to the mutants used as bait; thus, mutant A was tested against mutant A, etc. See also Fig. 6.

[b] Interactions involving Dpb2p were carried out with *DPB2* cloned in both binding domain and activation domain vectors. Dpb3p interaction with Pol2p mutants was only tested with *DPB3* in the activation domain vector, since there was no interaction between Dpb3p and wild-type Pol2p in either orientation.

minus of pol ϵ, although far removed from the catalytic domain, is essential for replication, for repair, and for DNA damage-induced transcription and cell cycle arrest. It has been proposed that pol ϵ could be involved in the initial recognition and processing of the DNA damage. How pol ϵ recognizes and communicates the checkpoint signal downstream to other member(s) of the transduction machinery is unknown. In this study, we have begun to illuminate the structural basis for the checkpoint function of pol ϵ by site-specific deletion mutagenesis of the C terminus. We demonstrate that amino acid residues (mutants E and F) between ZF1 and ZF2 in the C terminus are essential for viability, indicating a role in DNA replication. Furthermore, the temperature-sensitive *pol2* mutant F showed a significant loss in viability at the nonpermissive temperature and had partially elongated spindles when most of the cells were still in the S phase. The results are consistent with a role for these inter-zinc finger amino acids in coupling DNA replication and S/M checkpoint. Although we measured the checkpoint defects both in the presence and absence of HU, it is still not clear whether pol ϵ is part of a signal that restrains mitosis during a normal cell cycle or just part of the response to replication inhibition, since the checkpoint failure is not detectable at permissive temperatures. Recently, D'Urso and Nurse (30), by examining the phenotype of germinating spores containing a disruption of the *cdc20*$^+$ gene (encoding pol ϵ from *Schizosaccharomyces pombe*) showed that, contrary to expectations from previous studies of the effect of HU on *Saccharomyces cerevisiae pol2* mutants, *S. pombe* has a functional S phase checkpoint in the complete absence of pol ϵ. To explain this behavior, it was proposed that the checkpoint in the presence of DNA damage by HU might be different than the checkpoint for the coordination between the S and M phase in a normal cell cycle. This is entirely possible, since there are clearly numerous subsets of checkpoint pathways yet to be defined.

The S/M checkpoint cell cycle arrest pathway and damage-sensitive transcription induction pathway appear to share many common regulatory elements (1). *pol2–11* and *pol2–12* mutants with defects in the S phase checkpoint were also defective in recognizing MMS-induced DNA damage. *rfc5–1* mutants, defective in the DNA polymerase clamp loader, were also shown to have reduced damage-induced transcription and a defective S/M checkpoint (11, 31). In the current study, we show that *pol2-F* appears to share the same behavior. Mutant F was very sensitive to MMS and showed reduced *RNR3* induction in the presence of MMS, in addition to the cell cycle

effects discussed. Mutants A, B, C, and D, with deletions in ZF1, were less sensitive to growth on HU-containing plates than mutant F, but they were more sensitive to MMS and showed equivalent reduced expression of *RNR3*. The sensitivity toward MMS could also arise due to a direct defect in the DNA repair machinery, although it seems less likely since *pol2–11* and *pol2–12* mutants are proficient in the repair of MMS-induced damage (32).

Extensive genetic studies and biochemical analysis suggest that the 1200 C-terminal amino acids of *POL2* contain sites that stabilize subunit interactions in the pol ϵ holoenzyme complex (8, 18, 24, 25, 33). The data presented in this study support this by demonstrating interaction between the C terminus of the catalytic subunit and the conserved subunit, Dpb2p, using the two-hybrid assay. The C terminus is not sufficient for interaction with Dpb3p. However, the two-hybrid analysis also suggests that there may be an additional, previously unsuspected interaction involving this domain. Using amino acids 1265 to the stop codon of *POL2* as bait in the yeast two-hybrid assay, we found that the C terminus of wild-type pol ϵ cloned into the activation domain vector can efficiently activate transcription, whereas mutants E and F were unable to do so. Since mutants E and F are defective in replication, the two-hybrid assay results suggest that at least one essential form of pol ϵ is oligomeric, perhaps a dimer. We do not know if the interaction requires another yeast protein as a bridge, however, since two-hybrid assays with yeast proteins cannot distinguish direct from indirect protein/protein interactions. It is clear, however, that the same mutations that abolish the apparent homodimerization also weaken the interaction of Pol2p with Dpb2p. The proposed oligomerization could explain several other findings. The interallelic complementation of *pol2–11* and *pol2–18* mutants (9), the interallelic complementation of *pol2–18* and *pol2-F* mutations (this work), partial complementation of *pol2–11* by a C-terminal fragment of *POL2* (9), and, in *S. pombe*, the apparently dominant negative effect of expression of a mutant pol ϵ in *cdc20*Δ germinating spores (30) could all be explained if pol ϵ acts as a dimer. The possible dimerization of pol ϵ is also interesting in view of the fact that the *E. coli* DNA polymerase III holoenzyme, the essential replicase, forms dimers in solution and acts as a dimer during coordinated synthesis of the leading and lagging strands (34). Although it is thought that leading and lagging strand elongation are coordinated through the use of two different gene products, pol δ and pol ϵ, one on each strand, obviating the need for dimeric polymerases as are found in prokaryotes, a possible role for dimeric polymerases in eukaryotes could be coordination of the two forks emanating from a single origin. The idea that the two branch points of a bidirectional replication bubble are connected into a binary replisome was put forward many years ago as a mechanism to prevent rotation of the two forks with respect to each other and thus avoid undue tangling of the daughter chromosomes (35). Dimerization of the polymerases could both serve to link the two forks physically and to ensure synchronous activity at both forks. It has previously been suggested that DNA helicases may also have an organizational role in tethering diverging replication forks to each other (36).

Active replication complexes have been proposed to constitute a device that, once formed, continually sends an inhibitory signal to the checkpoint machinery to prevent mitosis until the replication phase (S phase) is faithfully completed (37). Disassembly after completion of replication would then allow mitosis. At which point in assembly is the surveillance mechanism activated? Does it require unwinding and conversion of the origin into a replication fork? Mutant F, described here, shows a correlation between a defective S/M phase checkpoint and destabilized protein-protein interactions, suggesting that the proper assembly of the pol ϵ complex within the replication complex could be important for initiating and/or maintaining the S phase checkpoint signal. pol ϵ has been shown to be absent from origin replication complexes early in G_1 and to associate with origin replication complexes late in G_1, so the periodic association of pol ϵ with origins would be consistent with a role in the checkpoint (38). It is still possible, however, that the protein-protein interactions are required only for the replication function of pol ϵ. In fact, in only one case have a replication defect and a checkpoint defect been (partially) genetically separated. The overexpression of the *POL30* gene, encoding the proliferating cell nuclear antigen was shown to suppress the replication defect of the *rfc5* but not its checkpoint defect (11).

Another mystery is how the whole assembly of proteins can sense incomplete DNA replication and DNA damage due to radiation or chemicals such as MMS in chromosomes undergoing replication. Something in the structure of the DNA itself, such as stretches of single-stranded DNA formed during replication and blocks due to DNA damage, has been proposed to act as a signal in the S phase, and the zinc finger of pol ϵ has been proposed to monitor the signal (9). Single-stranded DNA has been shown to act both as an efficient trap for pol ϵ and to actually promote dissociation of full-length pol ϵ but not a pol ϵ protein missing amino acids 1270 to the end (aa 2222) from primer-templates, suggesting that there is a binding site for single-stranded DNA in the large, non-catalytic C-terminal region (39). The mutant phenotypes described in this work suggest that the zinc finger region may be what is critical for single-stranded DNA sensing in that C-terminal segment. A damage recognition role has been proposed for zinc fingers in two other proteins (40). The new checkpoint-defective mutants will be useful in reconstituting mutant pol ϵ holoenzymes to further evaluate the physical mechanism of the sensing of DNA damage using *in vitro* binding studies and kinetic analysis of activity on various model substrates.

Acknowledgments—We thank the members of the Campbell laboratory for helpful discussions and Dr. Julie Archer for help in immunofluorescence studies. We are grateful to Akio Sugino and Hiroyuki Araki for pol ϵ antibodies and the *pol2* knock-out strain, YHA301.

REFERENCES

1. Lydall, D., and Weinert, T. (1995) *Science* **270,** 1488–1491
2. Murray, A. W. (1992) *Nature* **359,** 599–604
3. Paulovich, A. G., and Hartwell, L. H. (1995) *Cell* **82,** 841–847
4. Marini, F., Paciotti, V., Lucchini, G., Plevani, P., Stern, D. F., and Foiani, M. (1997) *EMBO J.* **16,** 639–650
5. Piatti, S., Lengauer, C., and Nasmyth, K. (1995) *EMBO J.* **14,** 3788–3799
6. Toyn, J. H., Johnson, A. L., and Johnston, L. H. (1995) *Mol. Cell. Biol.* **15,** 5312–5321
7. Humphrey, T., and Enoch, T. (1995) *Curr. Biol.* **5,** 376–379
8. Araki, H., Leem, S.-H., Amornrat, P., and Sugino, A. (1995) *Proc. Natl. Acad. Sci. U. S. A.* **92,** 11791–11795
9. Navas, T. A., Zhou, Z., and Elledge, S. J. (1995) *Cell* **80,** 29–39
10. Navas, T. A., Sanchez, Y., and Elledge, S. J. (1996) *Genes Dev.* **10,** 2632–2543
11. Sugimoto, K., Ando, S., Shimomura, T., and Matsumoto, K. (1997) *Mol. Cell. Biol.* **17,** 5905–5914
12. Noskov, V. N., Araki, H., and Sugino, A. (1998) *Mol. Cell. Biol.* **18,** 4913–492
13. Lydall, D., and Weinert, T. (1995) *Science* **270,** 1488–1491
14. Lydall, D., and Weinert, T. (1997) *Mol. Gen. Genet.* **256,** 638–651
15. Zhou, Z., and Elledge, S. J. (1993) *Cell* **75,** 1119–1127
16. Budd, M. E., and Campbell, J. L. (1993) *Mol. Cell. Biol.* **13,** 496–505
17. Budd, M. E., and Campbell, J. L. (1995) *Mol. Cell. Biol.* **15,** 2173–2179
18. Morrison, A., Araki, H., Clark, A. B., Hamatake, R. K., and Sugino, A. (1990) *Cell* **62,** 1143–1151
19. Araki, H., Ropp, P. A., Johnson, A. L., Johnston, L. H., Morrison, A., and Sugino, A. (1992) *EMBO J.* **11,** 733–740
20. Copeland, W. C., and Wang, T. S.-F. (1993) *J. Biol. Chem.* **268,** 11028–11040
21. Sikorski, R. S., and Hieter, P. (1989) *Genetics* **122,** 19–27
22. Budd, M., and Campbell, J. L. (1987) *Proc. Natl. Acad. Sci. U. S. A.* **84,** 2838–2842
23. James, P., Holladay, J., and Cragi, E. A. (1996) *Genetics* **144,** 1425–1436
24. Araki, H., Hamatake, R. K., Johnston, L. H., and Sugino, A. (1991) *Proc. Natl. Acad. Sci. U. S. A.* **88,** 4601–4605
25. Araki, H., Hamatake, R. K., Morrison, A., Johnston, L. H., and Sugino, A.

(1991) *Nucleic Acids Res.* **19,** 4867–4872
26. Allen, J. B., Zhou, Z., Siede, W., Frideberg, E. C., and Elledge, S. J. (1994) *Genes Dev.* **8,** 2416–2428
27. Berg, J. M. (1996) *Science* **271,** 1081–1085
28. Fields, S., and Song, O. K. (1989) *Nature* **340,** 245–246
29. James, P., Halladay, J., and Craig, E. A. (1996) *Genetics* **144,** 1425–1436
30. D'Urso, G., and Nurse, P. (1997) *Proc. Natl. Acad. Sci. U. S. A.* **94,** 12491–12496
31. Sugimoto, K., Shimomura, T., Hashimoto, K., Araki, H., Sugino, A., and Matsumoto, K. (1996) *Proc. Natl. Acad. Sci. U. S. A.* **93,** 7048–7052
32. Halas, A., Baranowska, H., Policinska, Z., and Jachmyczyk, W. J. (1997) *Curr. Genet.* **31,** 292–301
33. Sugino, A. (1995) *Trends Biochem.* **20,** 319–323
34. Yuzhakov, A., Turner, J., and O'Donnell, M. (1996) *Cell* **86,** 877–886
35. Sundin, O., and Varshavsky, A. (1980) *Cell* **21,** 103–114
36. Wessel, R., Schweizer, J., and Stahl, H. (1992) *J. Virol.* **66,** 804–815
37. Li, J. J., and Deshaies, R. (1993) *Cell* **7,** 223–226
38. Aparicio, O. M., Weinstein, D. M., and Bell, S. (1997) *Cell* **91,** 59–69
39. Maki, S., Hashimoto, K., Ohara, T., and Sugino, A. (1998) *J. Biol. Chem* **273,** 21332–21341
40. Jackson, S. P. (1997) *Curr. Opin. Genet. Devel.* **6,** 19–25
41. Srienc, F., Campbell, J. L., and Bailey, J. (1986a) *Cytometry* **7,** 132–141
42. Yoon, H.-J., and Campbell, J. L. (1991) *Proc. Natl. Acad. Sci. U. S. A.* **88,** 3574–3578
43. Johnson, L. M., Snyder, M., Chang, L. M. S., Davis, R. W., and Campbell, J. L. (1985) *Cell* **43,** 369–377